Am J Cancer Res 2023;13(10):4708-4720
www.ajcr.us /ISSN:2156-6976/ajcr0151173

Original Article

Sulforaphene suppresses oesophageal cancer growth through mitogen- and stress-activated kinase 2 in a PDX mouse model

Chengjuan Zhang[1,6*], Qiong Wu[2,11*], Ke Yao[9*], Guoguo Jin[3], Simin Zhao[4], Junxia Zhang[7], Wenjin Zheng[1], Benling Xu[8], Yingling Zu[5], Jing Yuan[1], Kangdong Liu[2,11], Yongjun Guo[10]

[1]Center of Bio-Repository, The Affiliated Cancer Hospital of Zhengzhou University, Henan Cancer Hospital, Zhengzhou, Henan, P. R. China; [2]Department of Pathophysiology, School of Basic Medical Sciences, Zhengzhou University, Zhengzhou, Henan, P. R. China; [3]Henan Key Laboratory of Chronic Disease Management, Fuwai Central China Cardiovascular Hospital, Zhengzhou, Henan, P. R. China; [4]Department of Pathology, The Affiliated Cancer Hospital of Zhengzhou University, Henan Cancer Hospital, Zhengzhou, Henan, P. R. China; [5]Department of Hematology, The Affiliated Cancer Hospital of Zhengzhou University, Henan Cancer Hospital, Zhengzhou, Henan, P. R. China; [6]Henan Key Laboratory of Molecular Pathology, Zhengzhou, Henan, P. R. China; [7]Academy of Chinese Medical Sciences, Henan University of Chinese Medicine, Zhengzhou, Henan, P. R. China; [8]Department of Immunotherapy, The Affiliated Cancer Hospital of Zhengzhou University, Henan Cancer Hospital, Zhengzhou, Henan, P. R. China; [9]Department of Cellular and Molecular Biology, University of Minnesota, Austin, MN, USA; [10]Department of Molecular Pathology, The Affiliated Cancer Hospital of Zhengzhou University, Henan Cancer Hospital, Zhengzhou, Henan, P. R. China; [11]China-US (Henan) Hormel Cancer Institute, Zhengzhou, Henan, P. R. China. [*]Equal contributors.

Received May 10, 2023; Accepted September 4, 2023; Epub October 15, 2023; Published October 30, 2023

Abstract: Background: Although sulforaphene has potential anticancer effects, little is known about its effect on oesophageal squamous cell carcinoma (ESCC) invasiveness. Methods: To investigate whether sulforaphene inhibits the growth of oesophageal cancer cells, MTT and anchorage-independent cell growth assays were performed. Global changes in the proteome and phosphoproteome of oesophageal cancer cells after sulforaphene treatment were analysed by mass spectrometry (MS), and the underlying molecular mechanism was further verified by in vivo and in vitro experiments. Results: Sulforaphene treatment markedly affected proteins that regulate several cellular processes in oesophageal cancer cells, and mitogen- and stress-activated kinase 2 (MSK2) was the main genetic target of sulforaphene in reducing the growth of oesophageal cancer cells. Sulforaphene significantly suppressed ESCC cell proliferation in vitro and reduced the tumour size in an oesophageal patient-derived xenograft (PDX) SCID mouse model. Furthermore, the binding of sulforaphane to MSK2 in vitro was verified using a cellular thermal dhift assay, and the effect of MSK2 knockdown on the ESCC phenotype was observed using a shMSK2 model. Conclusion: The results showed that sulforaphene suppresses ESCC growth in both human oesophageal squamous cells and PDX mouse model by inhibiting MSK2 expression, implicating sulforaphene as a promising candidate for ESCC treatment.

Keywords: Sulforaphene, oesophageal cancer, proliferation, mitogen-activated and stress-activated kinase 2 (MSK2), patient-derived xenograft mouse model (PDX)

Introduction

Oesophageal cancer is the ninth most common cancer and the sixth most common cause of cancer death globally [1, 2]. Oesophageal cancer has two major histological subtypes: oesophageal squamous cell carcinoma (ESCC) and oesophageal adenocarcinoma (EAC) [3, 4]. Between them, ESCC is the predominant histological type, accounting for 80% of all oesophageal cancer cases worldwide. The five-year survival rate for ESCC is only 15%-25% due to limited early clinical diagnostic and treatment methods.

Accumulating evidence indicates that dietary cruciferous vegetables are associated with low cancer risk [5]. The anticancer activity of cruciferous vegetables is mainly attributed to isocyanates (ITCs) [6], of which phenethyl ITC (PEITC),

allyl ITC, sulforaphane, and sulforaphene have chemopreventive and chemotherapeutic effects in vitro and in vivo [7, 8]. Broccoli contains a relatively high concentration of glucoraphanin, which is hydrolysed to produce sulforaphane [9]. Many studies have focused on sulforaphane as an anti-cancer agent in cruciferous plants. Sulforaphane has been identified to induce apoptosis in some cancer cell lines [10, 11]. However, the inhibitory activity of sulforaphene on gene mutation is 1.3-1.5 times that of sulforaphane [12, 13], and its toxicity to normal lymphocytes is very low [14]. Further, sulforaphene is abundant in *Raphanus sativus* seeds. Despite its promising potential, the anticancer effects and mechanism of action of sulforaphene have not been investigated in detail.

Here, we show that sulforaphene significantly suppresses ESCC cell proliferation and colony formation in vitro and inhibits tumour growth in vivo. Furthermore, according to phosphoproteome analysis, we show that Mitogen-activated and stress-activated kinase 2 (MSK2) is the target of sulforaphene in the inhibition of oesophageal squamous cell growth. MSKs are serine/threonine protein kinases activated by ERKs or p38 [15]. MSKs contain two kinase domains: an N-terminal kinase domain (NTKD) of the AGC kinase family and a C-terminal kinase domain (CTKD) of the calmodulin kinase family. ERK1/2 and p38 phosphorylate three MSK sites to activate CTKD. This leads to self-phosphorylation and activation of NTKD, and subsequent phosphorylation of the MSK substrate. The characteristic MSK substrates are histone H3 and the related transcription factors CREB and ATF1 [15]. MSKs phosphorylate CREB at Ser133, resulting in it being targeted by other kinases including protein kinase A (PKA) [16]. CREB phosphorylation creates a binding site for the co-activators CBP and P300 [17]. Several other matrices for MSK have been proposed, including NF-κB and HMG-14 [18, 19]. MSK2 is highly expressed in various cancer cell types and not only has a carcinogenic effect in cervical squamous cell carcinoma through the PAX8/RB-E2F1/cyclinA2 axis [20], but also acts as an anti-tumour proliferation and migration target in colon cancer [21]. MSK2 is also closely related to the occurrence and development of skin cancer and the expression of breast cancer marker genes [18, 22].

In this study, we observed the inhibitory effect of sulforaphane on the growth and proliferation of ESCC cells and conduct a series of proteomics and phosphorylomics experiments, as well as in vivo and in vitro studies, to further investigate the mechanism underlying sulforaphane's anti-oesophageal squamous cell carcinoma effect. The aims of this study was to provide a theoretical basis for sulforaphane as a candidate drug for ESCC treatment.

Materials and methods

Chemicals and reagents

Sulforaphene was purchased from Hangzhou Lin'an Tian Hong Technology Co., Ltd. The antibodies against MSK2 (1:1000 dilution, #ab99411), pMSK2 Thr568 (1:1000 dilution, bs-17855R), pCREB Ser133 (1:1000 dilution, #9198s, CST), pC-JUN Ser63 (1:1000 dilution, CST, #9261S), Tubulin (1:1000 dilution, #ab-7291) and Ki-67 (1:500, #bs-23103R) were obtained from Beijing Boorsen Biotechnology Co., Ltd.

Cell culture

Human oesophageal squamous cancer cells EC1 and Eca-109 were obtained from the Chinese Academy of Sciences (Shanghai, China). The cells were cultured in RPMI-1640 medium (HyClone, Beijing, China) supplemented with 10% fetal bovine serum (FBS, HyClone), 0.1 mg/ml streptomycin (North China Pharmaceutical Group Co., Shijiazhuang, Hebei, China) in a cell incubator at 37°C in a humidified air atmosphere containing 5% CO_2.

MTT assay

Cells (1×10^3-5×10^3 per well) were inoculated into 96-well plates with 100 μL per well of 10% FBS/RPMI-1640 medium to determine cell proliferation or cytotoxicity. After 24 h of culture, different concentrations of sulforaphene were added, and then the cells were collected at 24 h, 48 h and 72 h. MTT reagent (5 mg/mL; 10 μL) was added 4 h before collection during each treatment, followed by 15 min incubation with a crystal dissolving solution (0.1 mL; 0.04 N HCl in isopropanol). The absorbance at 570 nm was measured using a spectrophotometer to determine the cell proliferation activity.

Anchorage-independent cell growth assay

Cells (8×10^3) were suspended in 1 mL BME/10% FBS/0.33% agar with different concentrations of sulforaphene, and 3 mL solidified BME/10% FBS/0.5% agar of the same concentration was plated in each well of the 6-well plates. The culture was stored in a 5% CO_2 incubator at 37°C for 2 weeks, and the colony count was calculated under a microscope using the Image-Pro Plus software programme (Media Cybernetics, Inc., Rockville, MD).

Phosphopeptide enrichment and LC/MS assays

Phosphopeptide enrichment was carried out by prewashed antibody beads. Tryptic peptides were dissolved in NETN buffer (100 mM NaCl, 1 mM EDTA, 50 mM Tris-HCl, 0.5% NP-40, pH 8.0). The beads were washed four times with NETN buffer and twice with H_2O and were eluted from the beads with 0.1% trifluoroacetic acid. Finally, the eluted fractions were combined, dried and dissolved in 5% formic acid for LC-MS/MS analysis.

Enriched phosphopeptide samples were loaded onto a homemade reverse-phase analytical column (15-cm length, 75 μm i.d.) and eluted during a 1 h gradient (6% to 23% solvent B; 0.1% formic acid in 98% acetonitrile) over 26 min, 23% to 35% in 8 min and reaching 80% in 3 min then holding at 80% for the last 3 min. The peptides were subjected to NSI source followed by tandem mass spectrometry (MS/MS) in Q Exactive Plus connected online to the UPLC. The MS/MS data were processed using the MaxQuant search engine (v.1.5.2.8).

Lentiviral infection

The lentivirus packaging vectors (pMD2.0G and psPAX) were purchased from Addgene Inc. (Cambridge, MA). According to the manufacturer's protocol, to prepare 20 shRNA lentivirus particles, the lentivirus and packaging vector were transfected into HEK293T cells by using iMFectin poly DNA transfection reagent (GenDEPOT, Barker, TX). At 8 h after transfection, the culture solution was changed, and new cell medium was added to the culture for 36 h. Lentivirus particles were obtained by filtering with a 0.45 mm sodium acetate syringe filter. The particles were then mixed with 10 μg/mL polybrene (Millipore, Billerica, MA) to infect 60% of the fusion cells overnight. After 24 h, the culture medium was completely replaced by fresh growth medium, and cells were cultured for another 24 h with 1 μg/mL puromycin. Finally, cells were selected for the next experiment.

Two different sequences of MSK2 primers were designed, shMSK2-1CCGGCCAGACAGAGCAGAAGTATTTCTCGAGAAATACTTCTGCTCTGTCTGGTTTTTG (forward oligo sequence) and AATTCAAAAACCAGACAGAGCAGAAGTATTTCTCGAGAAATACTTCTGCTCTGTCTGG (reverse oligo sequence) and shMSK2-2CCGGCGAAATCATCCGTAGCAAGACCTCGAGGTCTTGCTACGGATGATTTCGTTTTTGG (forward oligo sequence) and AATTCAAAAACGAAATCATCCGTAGCAAGACCTCGAGGTCTTGCTACGGATGATTTCG (reverse oligo sequence). Finally, shMSK2-1 and shMSK2-2 transfected cells were selected for the next experiment.

Western blot analysis

Western blotting was performed to evaluate pMSK2, pCREB and pC-JUN protein expression levels. Cells were lysed on ice in ice-cold lysis buffer (RIPA:PMSF = 100:1) with a protease inhibitor cocktail. A bicinchoninic acid (BCA) assay kit (PC0020, Solarbio Science & Technology Co., Ltd., Beijing) was used to measure the protein concentration. We separated 35 μg of protein from each sample by SDS-PAGE and transferred the proteins to nitrocellulose membranes. After being blocked with non-fat milk for 2 h, the membranes were incubated with primary antibodies against pMSK2, pCREB, pC-JUN and Tubulin at 4°C overnight. Afterwards, the membranes were incubated with HRP-labeled anti-mouse or anti-rabbit secondary antibodies (1:10,000, Santa Cruz, Dallas, TX) at 15-25°C for 2 h. The immunoglobulins were then detected with a FluorChem imaging system (San Jose, CA) with the enhanced chemiluminescence (ECL) technique.

Cellular thermal shift assay

The cellular thermal shift assay (CESTA) was performed in the following manner. ESCC cells were inoculated into a 15 cm cell culture dish and cultured for 24 h. Afterwards, the medium containing Sulforaphene was replaced and

cells were then cultured for 1 h at 37°C. Cells were collected and washed twice with PBS before cell counting. The number of cells in each group was adjusted to 2×10^7 and then divided into 12 EP tubes. These tubes were transferred to a PCR apparatus and treated at different temperatures (37-70°C) for 3 min. The cells were then cleaved in liquid nitrogen and dissolved in ice. The cell suspension was centrifuged at 12,000 rpm for 10 min, the supernatant was absorbed and boiled with loading buffer for 5 min. SDS-PAGE was performed to detect the relative expression level of MSK2 protein.

Reporter gene activity

293T cells (5×10^4 per well) were seeded ionto 12-well dishes and incubated for 24 h. Cells were transfected with the AP-1 reporter plasmid (800 ng) and incubated for 36 h and then treated with sulforaphene for 24 h. Firefly luciferase activities were measured using substrates provided in the reporter assay system (Promega). Transfection efficiency was normalized with a Renilla plasmid as an internal control.

Patient-derived xenograft (PDX) model

This experiment was approved by the Zhengzhou University Institutional Animal Care and Use Committee (Zhengzhou, Henan, China). Fragments (2-3 mm) of solid tumours of oesophageal cancer patients (The Affiliated Cancer Hospital of Zhengzhou University) were implanted into immune-deficient mice to establish the PDX model. Mice were divided into the vehicle control group and the sulforaphene-treated (10 mg/kg) group (n = 8 mice per/group). On day 4 after tumour implantation, the control group mice were subcutaneously injected with 100 μL of PBS mixture (2% DMSO and 5% Tween-20 dissolved in PBS, prepared fresh every each time); the raphanin experimental group was injected subcutaneously with 100 μL of raphanin mixture (raphanin 10 mg/kg, 2% DMSO and 5% Tween-20 dissolved in PBS, which should be freshly prepared and used away from light), once a day for six weeks. Body weight and tumour volume were measured once a week and calculated based on the following formula: tumour volume (mm^3) = length × $width^2$ × 0.5.

Immunohistochemistry

Animal tissues were embedded in paraffin and cut into sections, and then the slides were stained by immunohistochemistry (IHC). The tissue was dealkylated and hydrated, and 0.5% Triton X-100 × PBS was used for 10 min. Next, the slices were incubated overnight at 4°C with Ki-67 and MSK2. Finally, sections were imaged by microscopy (100 ×) and analysed by Image-Pro Plus software (version 6.2) (Media Cybernetics).

Statistical analysis

Data are reported as the mean values ± standard deviation (S.D.). Each experiment was repeated at least 3 times independently, and the statistical methods included a one-way analysis of variance (ANOVA). A statistically significant difference was defined at $P < 0.05$.

Results

Sulforaphene inhibits the proliferation of oesophageal cancer cells

The chemical formula of sulforaphene, shown in **Figure 1A**, was obtained from a natural compound database. Oesophageal squamous cell carcinoma EC1 and Eca-109 cells were treated with different concentrations of sulforaphene (0, 5, 10 and 25 μM) and their proliferation was assessed via MTT assays. The results demonstrated that sulforaphene dramatically inhibited cell proliferation in a dose-dependent manner at both 48 and 72 h (**Figure 1B**). Additionally, the results of anchorage-independent cell growth assays showed that various concentrations of sulforaphene inhibited EC1 and Eca-109 cell clone formation on day 12 (**Figure 1C**).

Effects of sulforaphene treatment on cellular phosphorylation and proteomics

To explore the mechanisms underlying the inhibition of proliferation of esophageal squamous cancer cells by sulforaphene, we performed mass spectrometry (MS) to evaluate the phosphoproteome of EC1 cells after sulforaphene treatment. Quantitative proteomic analysis based on the SILAC strategy was performed (Supplementary Figure 1). The entire experiment was performed according to the workflow shown in **Figure 2A**. First, the cells were labelled

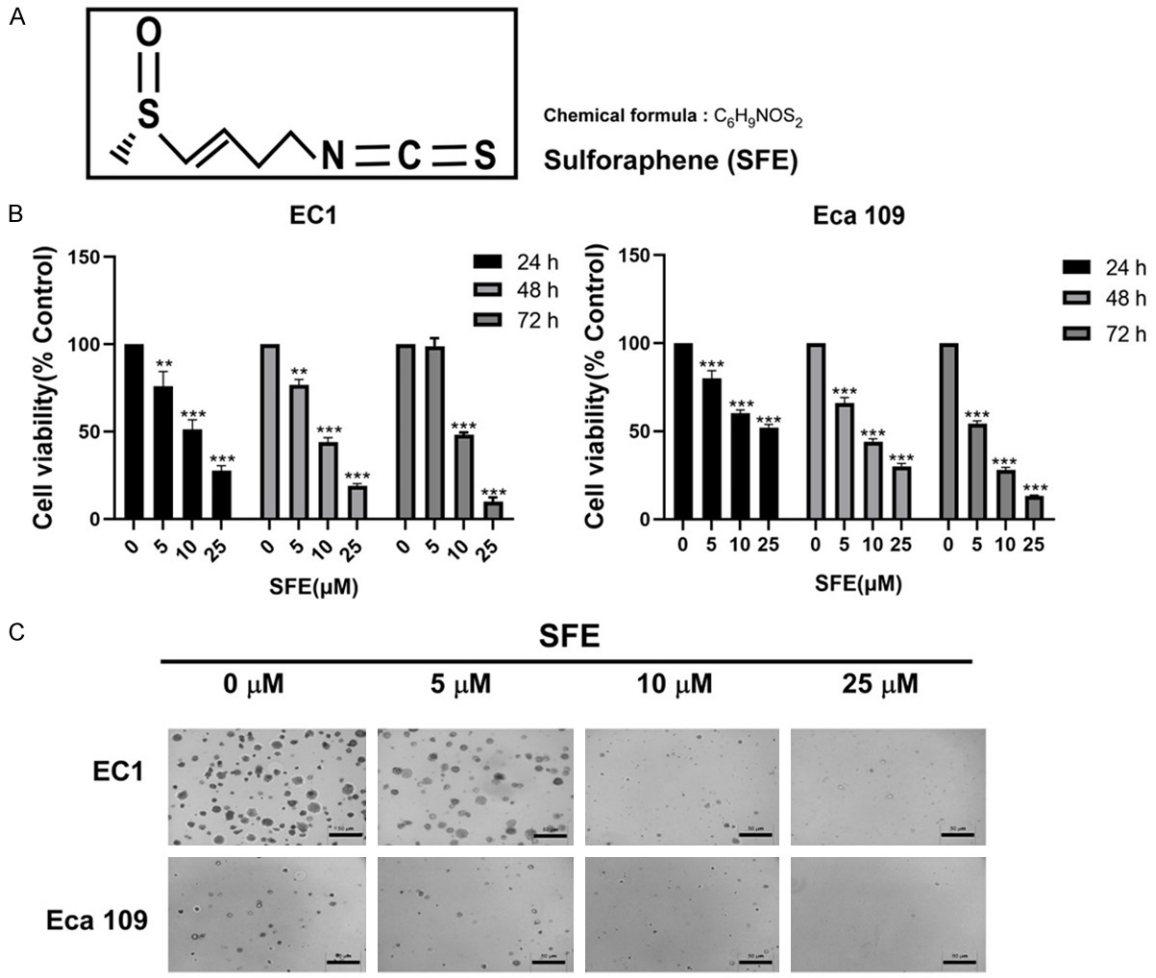

Figure 1. Sulforaphene (SFE) inhibits oesophageal cancer anchorage-independent cell growth and viability. A. Chemical structure of sulforaphene. B. EC1 and Eca-109 oesophageal cancer cells were treated with different concentrations of sulforaphene, and cell proliferation was determined by MTT assay. Sulforaphene significantly decreased the cell viability at 24 h, 48 h and 72 h. C. In the anchorage-independent cell growth assay, human oesophageal squamous cells EC1 and Eca-109 treated with 5, 10, and 25 μM sulforaphene showed inhibition of growth compared with the untreated group. Data are shown as the means ± S.D. from triplicate experiments. The asterisks (*) indicate significance ($P < 0.05$). **$P < 0.01$ vs. the 0 μM SFE group; ***$P < 0.001$ vs. the 0 μM SFE group.

with either "heavy isotopic amino acids" (L-13C6-Lysine/L-13C615N4-Arginine) or "light isotopic amino acids" (L-Lysine/L-Arginine), after which protein was extracted. We obtained the data through a series of steps, including enzymolysis, HPLC classification, affinity enrichment, and LC-MS. Finally, we analysed the data using a database search and bioinformatic analysis.

We identified 6989 phosphoric acid sites in 2824 proteins, of which 4461 sites in 1646 proteins contained quantitative information. We divided proteins into four groups, Q1 to Q4, according to their differential expression multiples: Q1 (0 < Ratio < 1/2), Q2 (1/2 < Ratio < 1/1.5), Q3 (1.5 < Ratio < 2), and Q4 (Ratio > 2). The distribution of phosphorylation sites following DMSO or sulforaphene treatment was analysed and the results are shown in **Figure 2B**. Overall, 76 modification sites were upregulated by 2-fold in the ESCC vs. the sulforaphene-treated cell group. In total, 244 modification sites exhibited values between 1.5- and 2-fold change, 78 modification sites were upregulated with fold change between 1/2- and 1/1.5-, and only 19 modification sites were upregulated with a fold change between 0- and 1/2- in the ESCC vs. the sulforaphene-treated group. Differentially phosphorylated

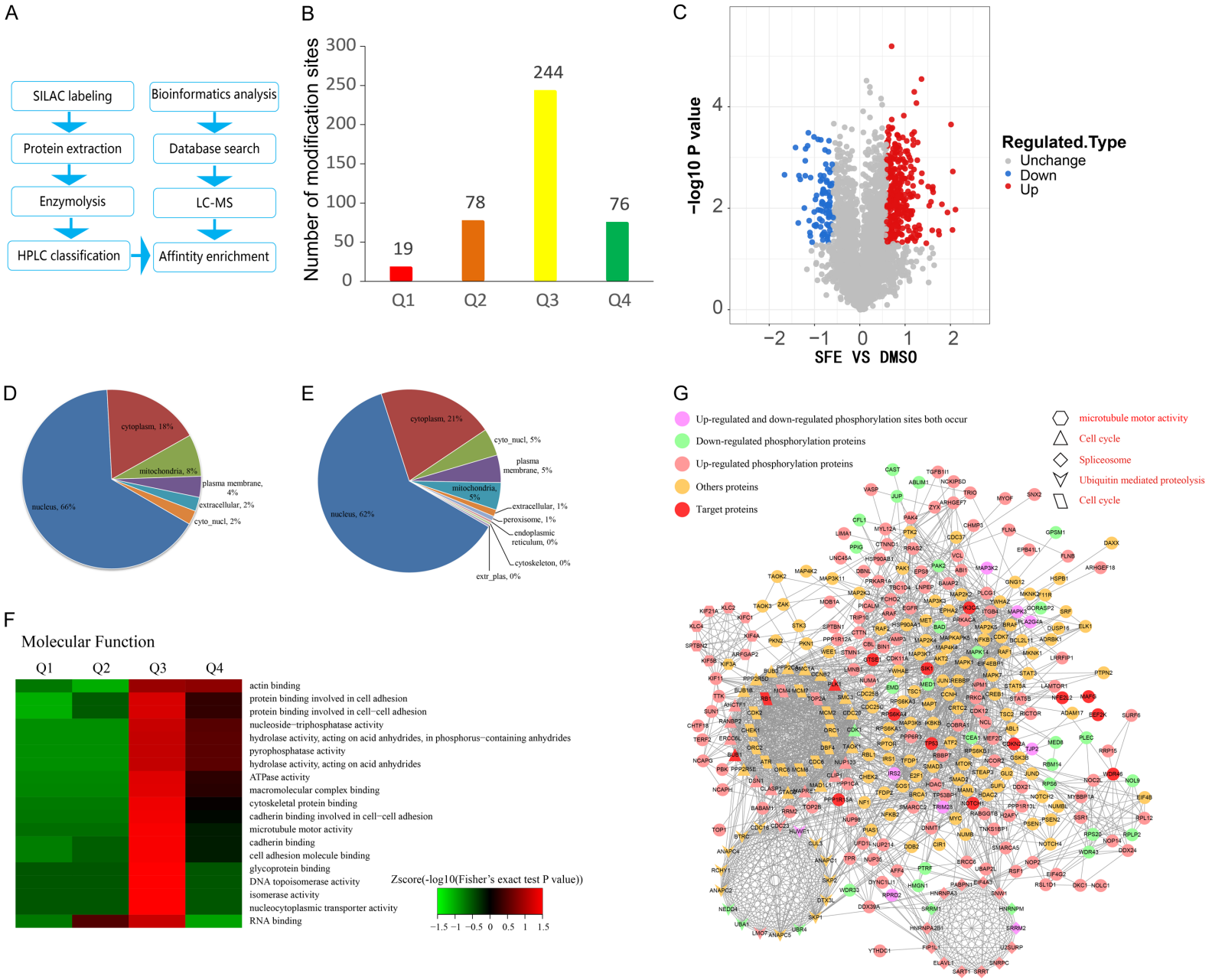
A
SILAC labeling
Protein extraction
Enzymolysis
HPLC classification
Bioinformatics analysis
Database search
LC-MS
Affintity enrichment
B
Number of modification sites
300
250
200
150
100
50
0
19
78
244
76
Q1
Q2
Q3
Q4
C
−log10 P value
4
2
0
−2
−1
0
1
2
SFE VS DMSO
Regulated.Type
Unchange
Down
Up
D
cytoplasm, 18%
mitochondria, 8%
plasma membrane, 4%
extracellular, 2%
cyto_nucl, 2%
nucleus, 66%
E
cytoplasm, 21%
cyto_nucl, 5%
plasma membrane, 5%
mitochondria, 5%
extracellular, 1%
peroxisome, 1%
endoplasmic reticulum, 0%
cytoskeleton, 0%
extr_plas, 0%
nucleus, 62%
F
Molecular Function
Q1
Q2
Q3
Q4
actin binding
protein binding involved in cell adhesion
protein binding involved in cell−cell adhesion
nucleoside−triphosphatase activity
hydrolase activity, acting on acid anhydrides, in phosphorus−containing anhydrides
pyrophosphatase activity
hydrolase activity, acting on acid anhydrides
ATPase activity
macromolecular complex binding
cytoskeletal protein binding
cadherin binding involved in cell−cell adhesion
microtubule motor activity
cadherin binding
cell adhesion molecule binding
glycoprotein binding
DNA topoisomerase activity
isomerase activity
nucleocytoplasmic transporter activity
RNA binding
Zscore(-log10(Fisher's exact test P value))
−1.5 −1 −0.5 0 0.5 1 1.5
G
Up-regulated and down-regulated phosphorylation sites both occur
Down-regulated phosphorylation proteins
Up-regulated phosphorylation proteins
Others proteins
Target proteins
microtubule motor activity
Cell cycle
Spliceosome
Ubiquitin mediated proteolysis
Cell cycle

Figure 2. Effects on cellular phosphorylation after sulforaphene (SFE) treatment, annotation and functional enrichment. A. The experimental routes of phosphoproteome analysis. B. The number distribution of phosphorylation sites upon DMSO or sulforaphene treatment in EC1 cells. Taking 1.5 times as the threshold, t-test *p*-value < 0.05 as the standard, Q1 means less than 1.5 times difference of proteins, Q4 means more than 1.5 times difference of proteins, Q2 and Q3 mean greater than 1.2 and less than 1.5 difference of upregulated and downregulated proteins, respectively. C. The global phosphorylation level analysis of EC1 cells upon DMSO or sulforaphene treatment. D. Pie chart of subcellular structure localization distribution of upregulated proteins. E. Pie chart of subcellular structure localization distribution of down-regulated proteins. F. GO analysis heat map of differentially phosphorylated proteins. Rows in the heat maps represent the enrichment test results of different comparison groups. The columns contain the description of enrichment-related functions (GO, KEGG pathway, protein domain). The differentially expressed proteins of different comparison groups and the corresponding colour blocks of functional descriptions indicate the degree of enrichment. Red represents a strong degree of enrichment, and green represents a weak degree of enrichment. G. Protein-protein interaction (PPI) network analysis of differentially phosphorylated proteins.

proteins between the DMSO- and sulforaphene-treated EC1 cells were identified from the volcano plot for global phosphorylation level analysis (**Figure 2C**).

Annotation and functional enrichment

GO and KEGG analyses were performed to profile the molecular and functional characteristics of differentially expressed proteins (Supplementary Figures 3, 5). All the identified proteins were categorised into 30 GO classifications, including 13 "biological processes", 9 "cellular components", and 8 "molecular functions". In addition, we used the WoLF PSORT software to predict the subcellular localisation of proteins and further classify differentially expressed proteins. We identified significantly altered proteins in various compartments of the cell, including the cytoplasm, nucleus, and extracellular space. The results showed that 66% of the downregulated phosphorylation site-related proteins were located in the nucleus (**Figure 2D**). Next, according to the *p*-value of the Fisher's exact test obtained by enrichment analysis, a hierarchical clustering method was used to identify the related functions of different groups and draw a heat map. Cluster analysis thermograms based on GO enrichment included three GO categories: biological processes, cellular components, and molecular functions (Supplementary Figures 2, 4). The results of the hierarchical clustering analysis are shown in **Figure 2E**.

Finally, differentially phosphorylated proteins as determined from MS were further analysed using protein-protein interaction (PPI) network analysis, All protein names and gene name identifiers were searched against the STRING database (version 10.5) for protein-protein interactions. According to the results of KEGG enrichment analyses, 18 pathways were significantly enriched, including "hsa04370 VEGF signalling pathway", and "hsa05145 Toxoplasmosis - Homo sapiens (human)" (**Figure 2F**). Most importantly, RPS6KA4 (MSK2), EEF2K, GTSE, and PPP1R15A were the main target proteins in the PPI network (**Figure 2G**). Phosphoproteomic analysis confirmed that sulforaphene treatment markedly affected proteins involved in the regulation of several cellular processes.

Sulforaphene suppresses cell proliferation by targeting MSK2

Based on the omics data, we selected 20 proteins that showed significant changes upon sulforaphene treatment. High-connotation screening was used to compare the effects of gene knockdown on the cell proliferation rate. Several genes with proliferation-inhibiting phenotypes were identified. Notably, the cell number in the MSK2 group was significantly lower on days 4 and 5 compared with that in the control (**Figure 3A**). Overall, these results suggest that sulforaphene inhibits oesophageal squamous cancer cell proliferation by targeting MSK2. To further investigate the role of MSK2 in oesophageal squamous carcinogenesis, we knocked down MSK2 expression in human oesophageal squamous cell lines using shRNA. MSK2 plays important roles in many cellular functions, including growth, proliferation, differentiation, inflammation, apoptosis, and malignant transformation. We examined the proliferation of cells treated with shRNAs targeting MSK2, finding decreased growth (**Figure 3B**, **3C**) alongside reduced MSK2 protein expression. Further, MTT assays from 24 to 96 h showed a significant decrease in cell viability (**Figure 3D**). We then examined the effect of MSK2 expression inhibition on the downstream signalling pathways. The phosphorylation levels of MSK2, CREB, and C-JUN

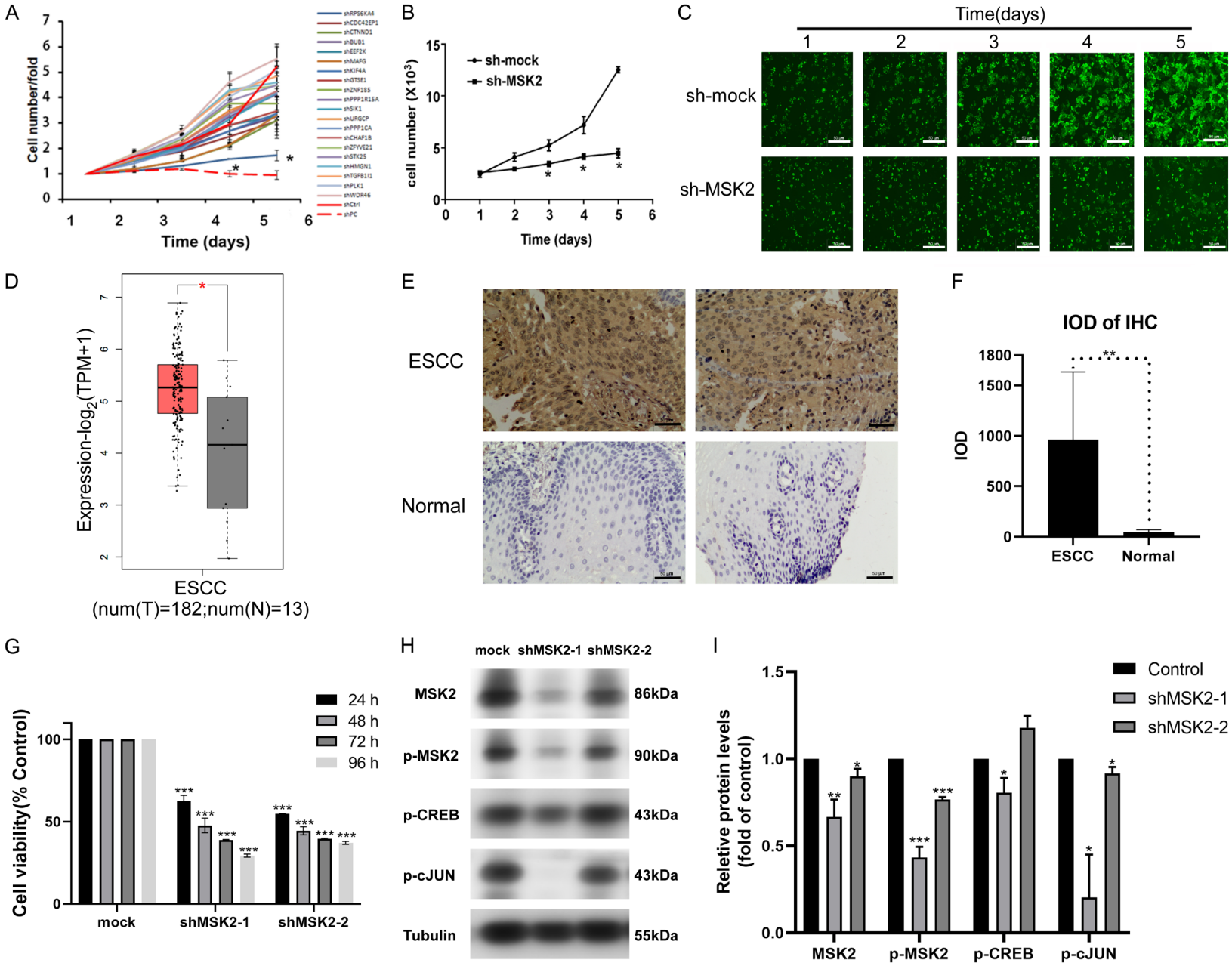
A
Cell number/fold
Time (days)
B
sh-mock
sh-MSK2
cell number (X10³)
Time (days)
C
Time(days)
1
2
3
4
5
sh-mock
sh-MSK2
D
Expression-log2(TPM+1)
ESCC
(num(T)=182;num(N)=13)
E
ESCC
Normal
F
IOD of IHC
IOD
ESCC
Normal
G
Cell viability(% Control)
24 h
48 h
72 h
96 h
mock
shMSK2-1
shMSK2-2
H
mock
shMSK2-1
shMSK2-2
MSK2
p-MSK2
p-CREB
p-cJUN
Tubulin
86kDa
90kDa
43kDa
43kDa
55kDa
I
Reletive protein levels (fold of control)
Control
shMSK2-1
shMSK2-2
MSK2
p-MSK2
p-CREB
p-cJUN

Figure 3. MSK2 is a potential therapeutic target in ESCC. A, B. The proliferation of cells was compared between the control group and the experimental groups (shRNA). C. Representative immunofluorescence images show that MSK2 knockdown inhibits the proliferation of oesophageal squamous cells. D. MSK2 mRNA level of ESCC cells in the database was higher than that of normal esophageal epithelial cells. E, F. The expression level of MSK2 in ESCC was significantly higher than that in normal esophageal epithelial tissues. ** indicates significant ($P < 0.01$). Data are shown as mean ± standard deviation for three replicates. G. The cell viability of two shMSK2 ESCC cell lines detected by MTT showed that the motility of ShMSK2-1 and ShmSK2-2 cells significantly decreased compared with mock at 24-96 h. ***$P < 0.0001$ compared with mock group. H, I. The phosphorylation levels of shMSK2-1 and shMSK2-2 MSK2 and MSK2/CREB/c-Jun were down-regulated compared with mock expression. *$P < 0.05$ compared with mock group; **$P < 0.001$ compared with mock group; ***$P < 0.0001$ compared with mock group.

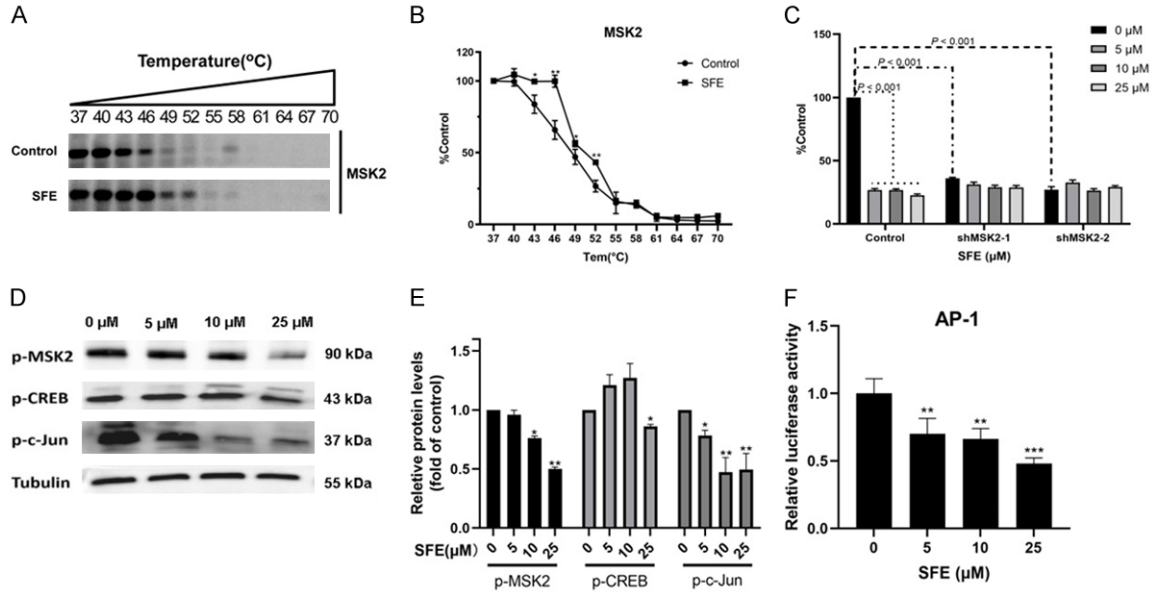

Figure 4. Sulforaphene (SFE) inhibits ESCC cell growth in a MSK2 dependent manner. A, B. CESTA experiment verified the binding of SFE to MSK2. * means significant ($P < 0.05$), ** means significant ($P < 0.01$). C. Effect of SFE concentration on cell viability of shMSK2-1 and shMSK2-2. Compared with Control group, the cell viability of shMSK2-1 and shMSK2-2 was decreased significantly ($P < 0.001$), but there was no statistical significance in shMSK2-1 and shMSK2-2 concentration of SFE groups compared with 0 μM ($P > 0.05$). D, E. Quantitative data were used to analyze the phosphorylation levels of indicator proteins of MSK2, CREB and C-JUN by Western blotting. Compared with 0 μM, * means significant ($P < 0.05$), ** means significant ($P < 0.01$). F. AP-1 activity was detected with different concentrations of sulforaphane. Compared with 0 μM, ** means significant ($P < 0.01$) and *** means significant ($P < 0.001$).

decreased at the same time as the level of MSK2 protein decreased (**Figure 3E**, **3F**). In addition, gene expression data relating to oesophageal squamous cell carcinoma were obtained from the cancer genome atlas (TCGA) database and analysed using GEPIA (http://gepia.cancer-pku.cn/). The results showed that MSK2 mRNA levels were higher in ESCC cells than in normal oesophageal epithelial cells (**Figure 3G**). We verified these expression differences using IHC and observed the expression of MSK2 protein in human ESCC tissues was significantly higher than that in normal oesophageal epithelial tissues (**Figure 3H**, **3I**).

To further verify the role of MSK2 in the inhibition of oesophageal squamous cell proliferation by sulforaphene, the binding of sulforaphene to MSK2 in ESCC cells was verified using the CESTA (**Figure 4A**, **4B**). In addition, the MTT results showed that when MSK2 was downregulated, the growth-inhibitory effect of sulforaphene on ESCC cells was diminished (**Figure 4C**). We also observed downregulation of the phosphorylation levels of proteins in the MSK2/CREB/c-Jun pathway in ESCC cells treated with different concentrations of sulforaphene (**Figure 4D**, **4E**). In addition, the activity of AP-1 (consisting of c-Jun and c-Fos)

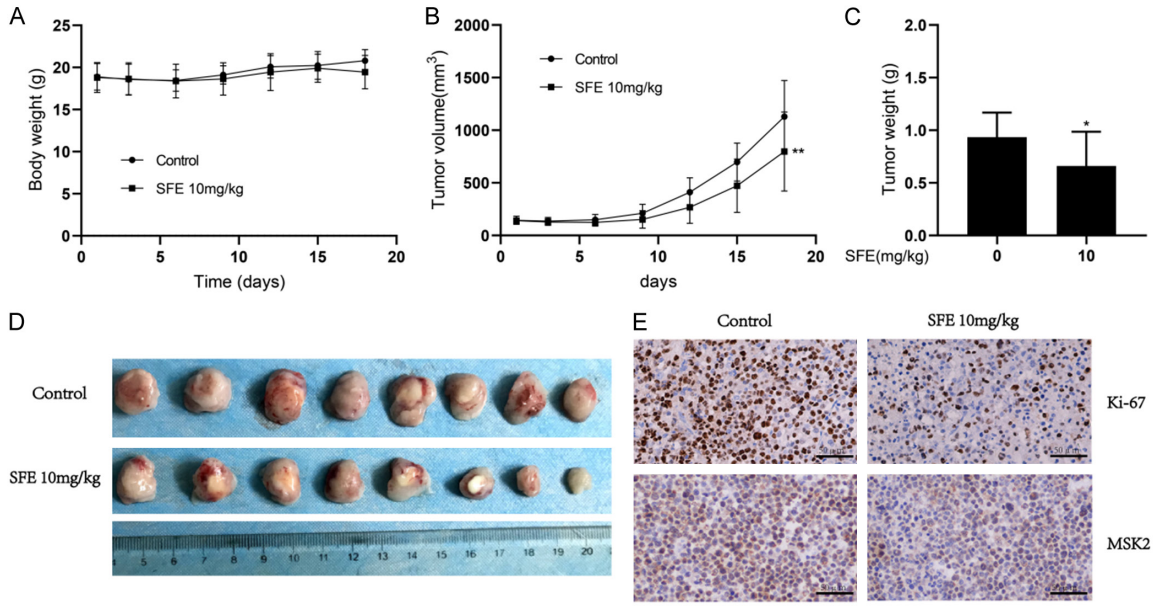

Figure 5. Sulforaphene (SFE) suppresses oesophageal PDX tumour growth. A. Sulforaphene treatment had no effect on the body weight of mice. B-D. Treatment with sulforaphene dramatically inhibited esophageal PDX growth and tumour weight compared with untreated group. E. Immunohistochemistry (IHC) staining of Ki-67 and MSK2. Representative images for each protein and each group are shown. Data are shown as the mean values ± S.D. from triplicate experiments. The asterisks (*) indicate significance ($P < 0.05$).

decreased after treatment with different concentrations of sulforaphene (**Figure 4F**).

Sulforaphene suppresses oesophageal tumour growth in a PDX mouse model

Finally, we used tumour tissues from patients with oesophageal cancer patients to generate patient-derived xenografts (PDXs). The results showed that sulforaphene (at 10 mg/kg) effectively inhibited tumour growth compared with the vehicle-treated group and decreased tumour weight compared with the control group (**Figure 5B-D**). No apparent loss in body weight was observed in the groups treated with various doses of sulforaphene, suggesting minimal toxicity (**Figure 5A**). Ki-67 and MSK2 levels were assessed with IHC in the vehicle and sulforaphene (10 mg/kg) groups, with sulforaphene treatment suppressing the Ki-67 and MSK2 levels (**Figure 5E**). And **Figure 6** illustrated the mechanism of sulforaphene inhibiting the proliferation of esophageal cancer cells.

Discussion

In this study, we assessed the effects of sulforaphene on ESCC. We showed that sulforaphene suppressed the proliferation of oesophageal cancer cells over 24, 48, and 72 h periods. Furthermore, we found that MSK2 might be a potential target for sulforaphene, as demonstrated by proteomic analysis of phosphorylation, representing a possible mechanism for the inhibition of proliferation on ESCC cells. Notably, sulforaphene also suppressed oesophageal tumour growth in the PDX mouse model. These novel findings indicate that sulforaphene is a promising novel agent for the treatment of oesophageal cancer and that MSK2 may be a potential therapeutic target for ESCC.

Epidemiological studies indicated that a high dietary intake of isothiocyanate, which is found in fruits and vegetables, is associated with lower cancer incidence [23]. One such isothiocyanate, sulforaphane, is considered a promising chemopreventive agent against cancer [24]. Sulforaphane can limit the progression of tumour development through a number of mechanisms, including activation of apoptosis [25], NF-κB pathway inhibition [26] and cell cycle arrest induction [27]. With continuous improvement in the understanding of tumour biology, the efficacy and toxicity of targeted drugs are also increasing, leading to these drugs being the first choice for clinical treatment due to their effects on angiogenesis,

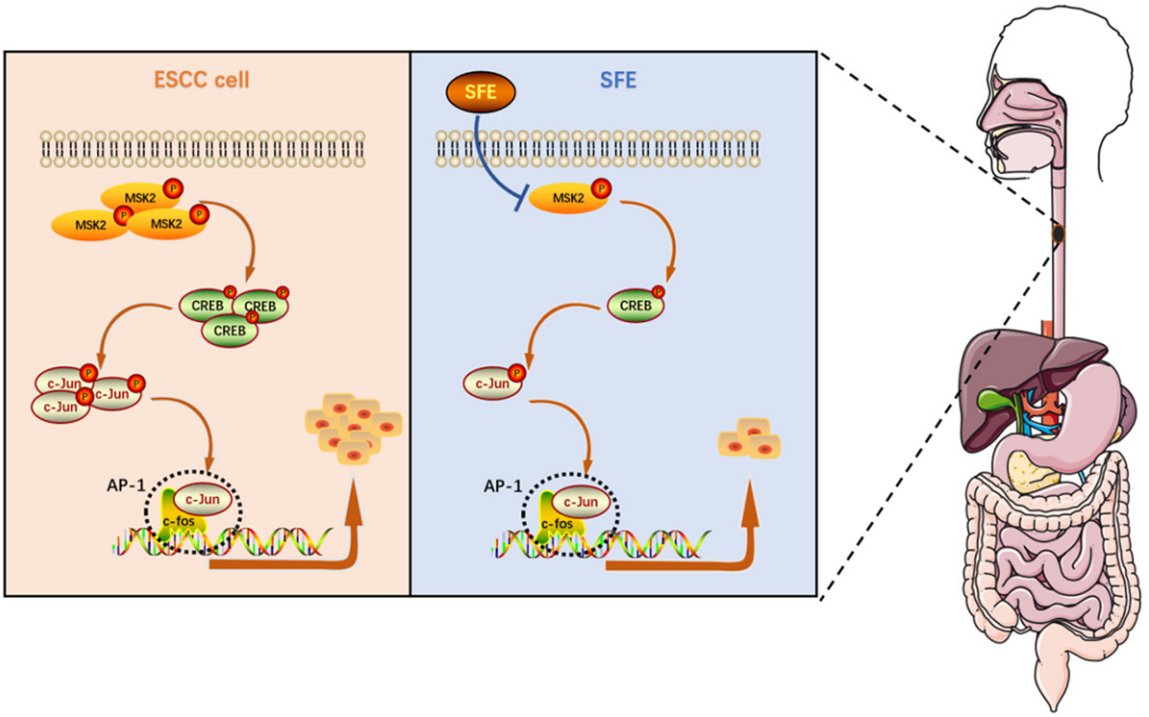

Figure 6. Schematic diagram of action of sulforaphene (SFE) in ESCC cells.

inflammation [28-30], cell cycle control [31], and apoptosis [32]. MSK2 is a nuclear kinase that acts downstream of ERK and p38 [33]. Activation of the Ras-MAPK pathway and MSK2, resulting in elevated H3 phosphorylation, may contribute to the aberrant gene expression observed in oncogene-transfected cells [34, 35].

In recent years, proteomic analysis in ESCC has been published, but has mainly been limited to studies of advanced stages [36]. In this study, we report the detailed proteome of ESCC cells treated with sulforaphene, using SILAC labelling and LC-MS/MS analyses. The inhibitory effect of sulforaphene on tumour proliferation places it as a promising therapeutic to reduce the mortality and morbidity of ESCC. Using phosphoproteomic analysis, we found that sulforaphene treatment markedly affected proteins involved in the regulation of several cellular processes. We further verified that MSK2 is a potential target of sulforaphene in the inhibition of the proliferation of ESCC cells. The results of this study showed that downregulation of MSK2 by shRNA effectively inhibited the proliferation of oesophageal squamous cells and inhibited the phosphorylation of proteins involved in the MSK2/CREB/c-Jun signalling pathway. Meanwhile, after MSK2 was downregulated, sulforaphene lost its inhibitory effect on oesophageal squamous cells or the phosphorylation of MSK2/CREB/c-Jun and the activity of AP-1 (composed of c-Jun and c-Fos). These data strongly suggest that MSK2 plays an important role in oesophageal squamous cell growth.

In this study, we observed that sulforaphene suppressed the viability of oesophageal squamous cells, concomitant with a reduction in colony formation in vitro and tumour growth in a PDX model. In addition, there was no obvious effect on the weight of the sulforaphene-treated mice in the PDX model. However, further, explicit toxicity analysis of sulforaphene is needed to identify unwanted side effects before entering clinical trials.

Conclusions

Overall, our results showed that sulforaphene exerted excellent inhibitory effects on oesophageal squamous carcinogenesis by directly targeting MSK2/CREB/C-JUN. Thus, sulforaphene may provide beneficial effects to prevent oesophageal cancer.

Acknowledgements

We would like to thank the PTM BioLab, Inc. for the analysis of proteomics and phosphorylation in this research. This work was supported by The Major public welfare projects of Henan Province - Research and development of new technologies for tumor liquid biopsy and immunotherapy (201300310400), The Key research and promotion special project of Henan province (Science and technology research) (202102310089), The Health Science and Technology Innovation Project for Young people of Henan Provincial (YXKC2021032), and Major science and technology project of Henan Province (221100310100).

Disclosure of conflict of interest

None.

Address correspondence to: Yongjun Guo, Department of Molecular Pathology, The Affiliated Cancer Hospital of Zhengzhou University, Henan Cancer Hospital, Zhengzhou 450008, Henan, P. R. China. Tel: +86-371-65587506; E-mail: yongjunguo@hotmail.com

References

[1] Napier KJ, Scheerer M and Misra S. Esophageal cancer: a review of epidemiology, pathogenesis, staging workup and treatment modalities. World J Gastrointest Oncol 2014; 6: 112-20.

[2] Lagergren J and Lagergren P. Oesophageal cancer. BMJ 2010; 341: c6280.

[3] Burki TK. Definitions of oesophageal cancer. Lancet Oncol 2017; 18: e71.

[4] Rustgi AK and El-Serag HB. Esophageal carcinoma. N Engl J Med 2014; 371: 2499-509.

[5] Abdull Razis AF and Noor NM. Cruciferous vegetables: dietary phytochemicals for cancer prevention. Asian Pac J Cancer Prev 2013; 14: 1565-1570.

[6] Abbaoui B, Lucas CR, Riedl KM, Clinton SK and Mortazavi A. Cruciferous vegetables, isothiocyanates, and bladder cancer prevention. Mol Nutr Food Res 2018; 62: e1800079.

[7] Singh SV and Singh K. Cancer chemoprevention with dietary isothiocyanates mature for clinical translational research. Carcinogenesis 2012; 33: 1833-1842.

[8] Kuang P, Song D, Yuan Q, Lv X, Zhao D and Liang H. Preparative separation and purification of sulforaphene from radish seeds by high-speed countercurrent chromatography. Food Chem 2013; 136: 309-315.

[9] Tortorella SM, Royce SG, Licciardi PV and Karagiannis TC. Dietary sulforaphane in cancer chemoprevention: the role of epigenetic regulation and HDAC inhibition. Antioxid Redox Signal 2015; 22: 1382-1424.

[10] Geng Y, Zhou Y, Wu S, Hu Y, Lin K, Wang Y, Zheng Z and Wu W. Sulforaphane induced apoptosis via promotion of mitochondrial fusion and ERK1/2-mediated 26S proteasome degradation of novel pro-survival bim and up-regulation of bax in human non-small cell lung cancer cells. J Cancer 2017; 8: 2456-2470.

[11] Zhang Z, Li C, Shang L, Zhang Y, Zou R, Zhan Y and Bi B. Sulforaphane induces apoptosis and inhibits invasion in U251MG glioblastoma cells. Springerplus 2016; 5: 235.

[12] Papi A, Orlandi M, Bartolini G, Barillari J, Iori R, Paolini M, Ferroni F, Grazia Fumo M, Pedulli GF and Valgimigli L. Cytotoxic and antioxidant activity of 4-methylthio-3-butenyl isothiocyanate from Raphanus sativus L. (Kaiware Daikon) sprouts. J Agric Food Chem 2008; 56: 875-883.

[13] Shi S and Kaur IP. Inhibition of cooked food-induced strangeness by dietary constituents: comparison of two natural idioticalness. Food Chem 2008; 112: 977-981.

[14] Wang L, Jiang H, Qiu Y, Dong Y, Hamouda HI, Balah MA and Mao X. Biochemical characterization of a novel myrosinase rmyr from rahnella inusitata for high-level preparation of sulforaphene and sulforaphane. J Agric Food Chem 2022; 70: 2303-2311.

[15] Karelina K, Liu Y, Alzate-Correa D, Wheaton KL, Hoyt KR, Arthur JS and Obrietan K. Mitogen and stress-activated kinases 1/2 regulate ischemia-induced hippocampal progenitor cell proliferation and neurogenesis. Neuroscience 2015; 285: 292-302.

[16] Naqvi S, Martin KJ and Arthur JS. CREB phosphorylation at Ser133 regulates transcription via distinct mechanisms downstream of cAMP and MAPK signalling. Biochem J 2014; 458: 469-479.

[17] Du Y, Teng X, Wang N, Zhang X, Chen J, Ding P, Qiao Q, Wang Q, Zhang L, Yang C, Yang Z, Chu Y, Du X, Zhou X and Hu W. NF-κB and enhancer-binding CREB protein scaffolded by CREB-binding protein (CBP)/p300 proteins regulate CD59 protein expression to protect cells from complement attack. J Biol Chem 2014; 289: 2711-2724.

[18] Khan P, Drobic B, Pérez-Cadahía B, Healy S, He S and Davie JR. Mitogen- and stress-activated protein kinases 1 and 2 are required for maximal trefoil factor 1 induction. PLoS One 2013; 8: e63189.

[19] Christian F, Smith EL and Carmody RJ. The regulation of NF-κB subunits by phosphorylation. Cells 2016; 5: 12.
[20] Wu Y, Li H, Wang H, Zhang F, Cao H and Xu S. MSK2 promotes proliferation and tumor formation in squamous cervical cancer via PAX8/RB-E2F1/cyclin A2 axis. J Cell Biochem 2019; 120: 11432-11440.
[21] Jin G, Yan M, Liu K, Yao K, Chen H, Zhang C, Yi Y, Reddy K, Gorja DR, Laster KV, Guo Z and Dong Z. Discovery of a novel dual-target inhibitor against RSK1 and MSK2 to suppress growth of human colon cancer. Oncogene 2020; 39: 6733-6746.
[22] Chang S, Iversen L, Kragballe K, Arthur JS and Johansen C. Mice lacking MSK1 and MSK2 show reduced skin tumor development in a two-stage chemical carcinogenesis model. Cancer Invest 2011; 29: 240-245.
[23] Zhang Y. Allyl isothiocyanate as a cancer chemopreventive phytochemical. Mol Nutr Food Res 2010; 54: 127-135.
[24] Ullah MF. Sulforaphane (SFN): an isothiocyanate in a cancer chemoprevention paradigm. Medicines (Basel) 2015; 2: 141-156.
[25] Suppipat K, Park CS, Shen Y, Zhu X and Lacorazza HD. Sulforaphane induces cell cycle arrest and apoptosis in acute lymphoblastic leukemia cells. PLoS One 2012; 7: e51251.
[26] Negi G, Kumar A and Sharma SS. Nrf2 and NF-κB modulation by sulforaphane counteracts multiple manifestations of diabetic neuropathy in rats and high glucose-induced changes. Curr Neurovasc Res 2011; 8: 294-304.
[27] Bryant CS, Kumar S, Chamala S, Shah J, Pal J, Haider M, Seward S, Qazi AM, Morris R, Semaan A, Shammas MA, Steffes C, Potti RB, Prasad M, Weaver DW and Batchu RB. Sulforaphane induces cell cycle arrest by protecting RB-E2F-1 complex in epithelial ovarian cancer cells. Mol Cancer 2010; 9: 47.
[28] Ayyappan S, Prabhakar D and Sharma N. Epidermal growth factor receptor (EGFR)-targeted therapies in esophagogastric cancer. Anticancer Res 2013; 33: 4139-4155.
[29] Todoric J, Antonucci L and Karin M. Targeting inflammation in cancer prevention and therapy. Cancer Prev Res (Phila) 2016; 9: 895-905.
[30] Eng L, Azad AK, Habbous S, Pang V, Xu W, Maitland-van der Zee AH, Savas S, Mackay HJ, Amir E and Liu G. Vascular endothelial growth factor pathway polymorphisms as prognostic and pharmacogenetic factors in cancer: a systematic review and meta-analysis. Clin Cancer Res 2012; 18: 4526-4537.
[31] Dominguez-Brauer C, Thu KL, Mason JM, Blaser H, Bray MR and Mak TW. Targeting mitosis in cancer: emerging strategies. Mol Cell 2015; 60: 524-536.
[32] Hassan M, Watari H, AbuAlmaaty A, Ohba Y and Sakuragi N. Apoptosis and molecular targeting therapy in cancer. Biomed Res Int 2014; 2014: 150845.
[33] Sever R and Brugge JS. Signal transduction in cancer. Cold Spring Harb Perspect Med 2015; 5: a006098.
[34] Kim HG, Lee KW, Cho YY, Kang NJ, Oh SM, Bode AM and Dong Z. Mitogen- and stress-activated kinase 1-mediated histone H3 phosphorylation is crucial for cell transformation. Cancer Res 2008; 68: 2538-2547.
[35] Vermeulen L, Vanden Berghe W, Beck IM, De Bosscher K and Haegeman G. The versatile role of MSKs in transcriptional regulation. Trends Biochem Sci 2009; 34: 311-318.
[36] Qi YJ, Chao WX and Chiu JF. An overview of esophageal squamous cell carcinoma proteomics. J Proteomics 2012; 75: 3129-3137.

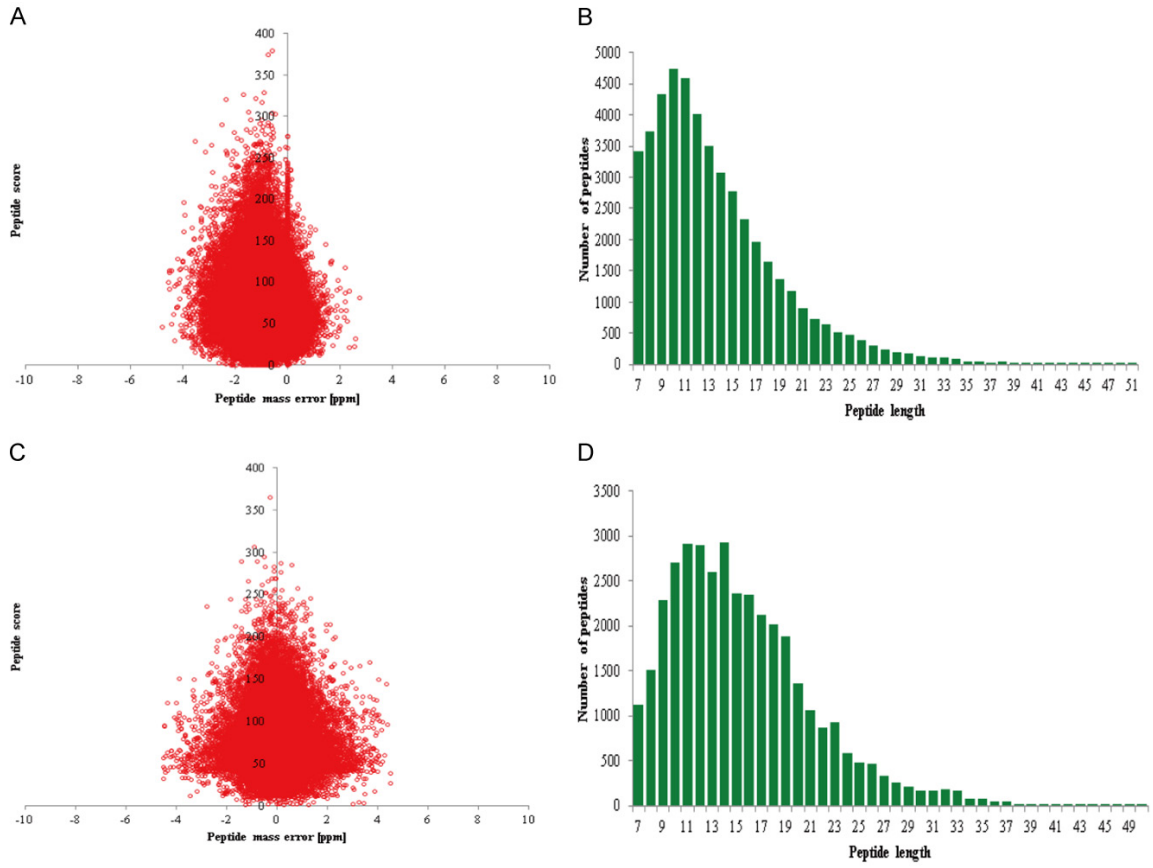

Supplementary Figure 1. Quality control test results of mass spectrum data. The mass shift distribution of peptides (A) and the length distribution of peptides (B) of Proteomics, The mass shift distribution of peptides (C) and the length distribution of peptides (D) of protein phosphorylomics.

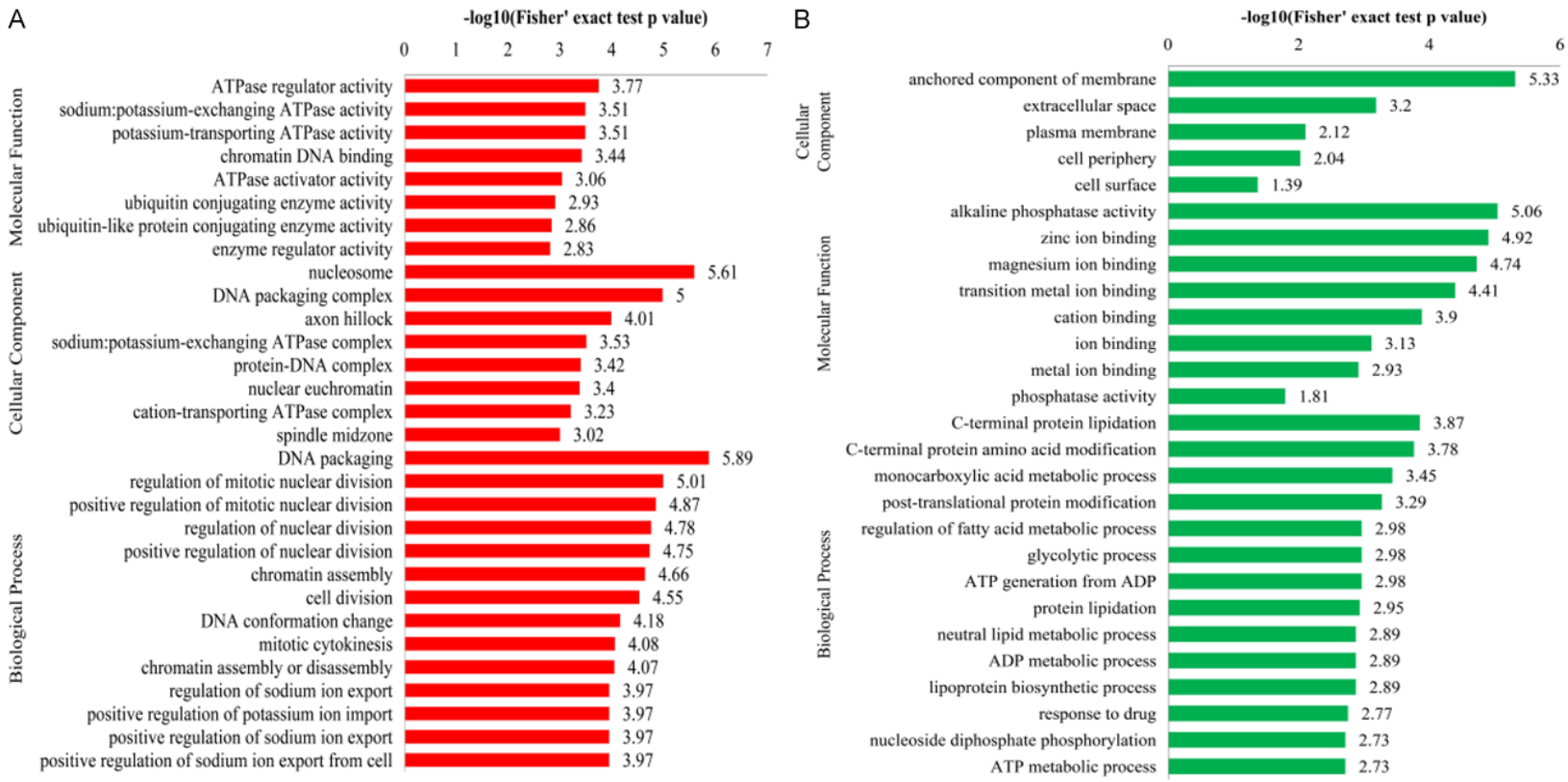

Supplementary Figure 2. Results of enrichment analysis of biological process, cellular component and molecular function in GO annotation of proteomics. GO enrichment results of up-regulated protein (A) and down-regulated protein (B) (EC1-SFEN/EC1-DMSO). *P*-values with statistical significance ($P < 0.05$) are present in the horizontal axis after a negative logarithmic transformation.

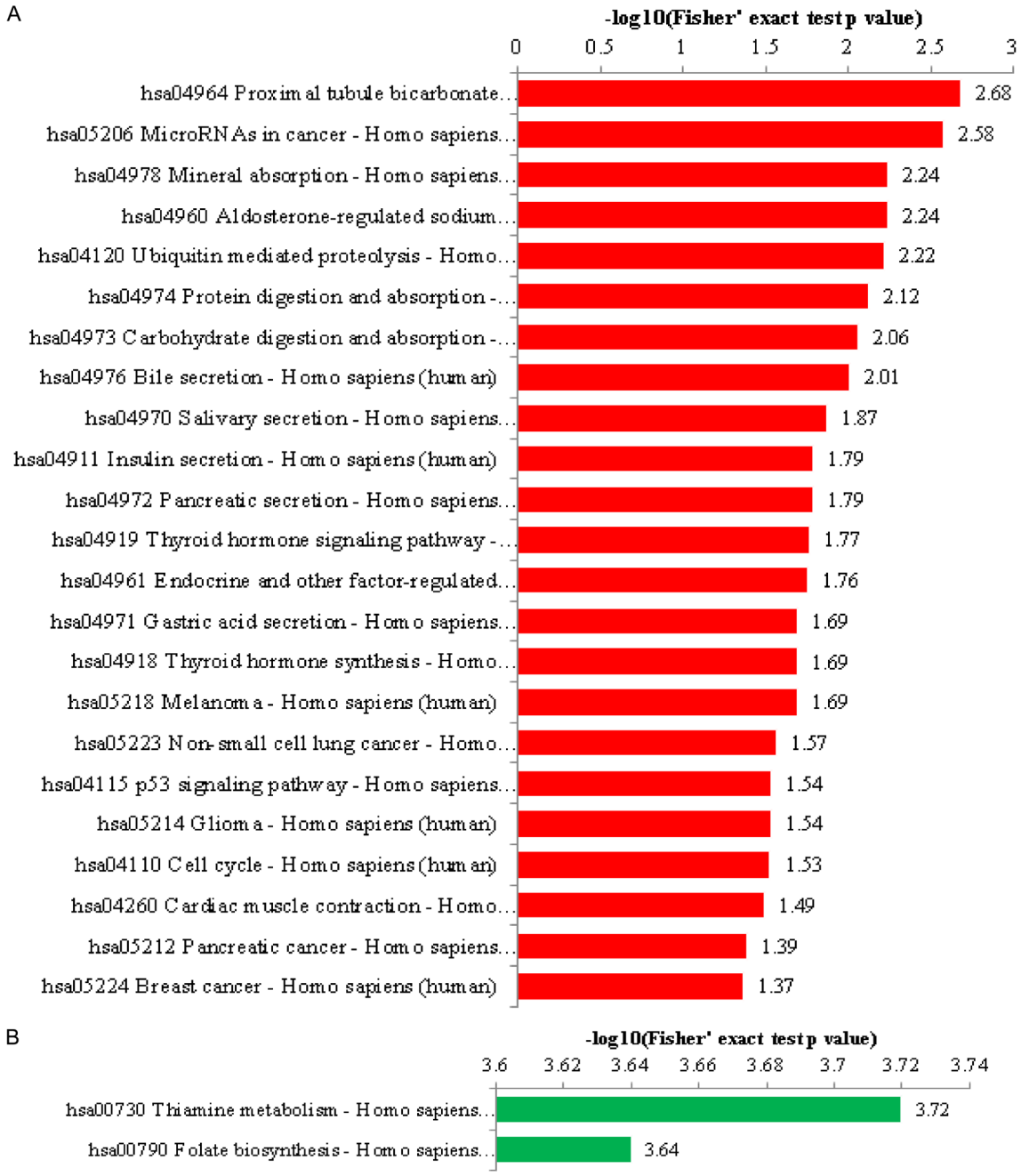

Supplementary Figure 3. Results of enrichment analysis of KEGG annotation of proteomics. KEGG enrichment results of up-regulated protein (A) and down-regulated protein (B) (EC1-SFEN/EC1-DMSO). *P*-values with statistical significance ($P < 0.05$) are present in the horizontal axis after a negative logarithmic transformation.

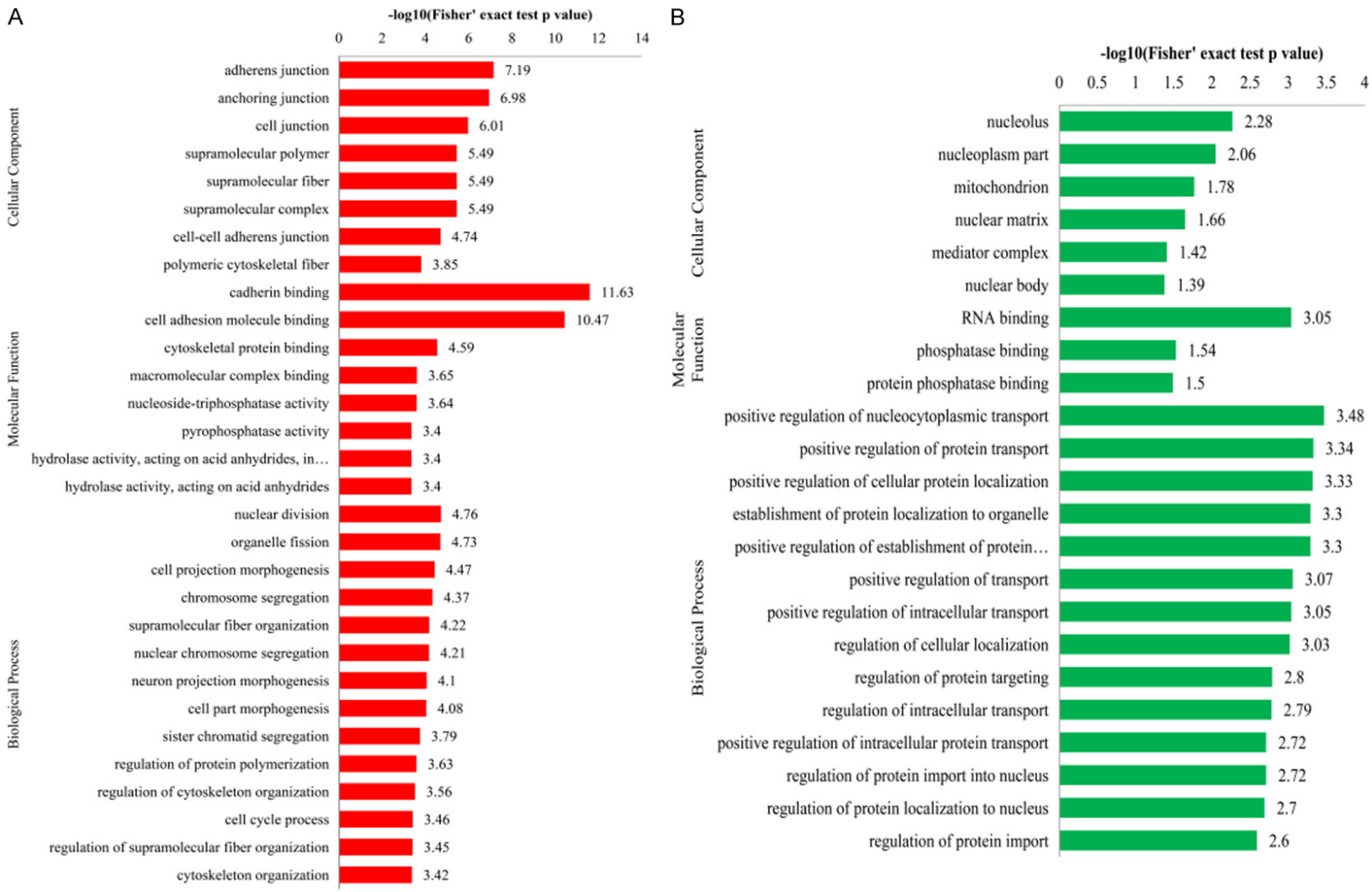

Supplementary Figure 4. Results of enrichment analysis of biological process, cellular component and molecular function in GO annotation of protein phosphorylomics. GO enrichment results of up-regulated protein (A) and down-regulated protein (B) (EC1-SFEN/EC1-DMSO). *P*-values with statistical significance ($P < 0.05$) are present in the horizontal axis after a negative logarithmic transformation.

Supplementary Figure 5. Results of enrichment analysis of KEGG annotation of protein phosphorylomics. KEGG enrichment results of up-regulated protein (A) and down-regulated protein (B) (EC1-SFEN/EC1-DMSO). *P*-values with statistical significance ($P < 0.05$) are present in the horizontal axis after a negative logarithmic transformation.